Thermomechanical Effects due to Hot Rolling Contact on the Energy Release Rates of Multiple Interface Cracks in Layered Media*

Takahito GOSHIMA**, Sotomi ISHIHARA**,
Nobuyasu YAMAUCHI** and Takashi KOIZUMI***

This paper deals with the mutual interference of multiple two-dimensional interface cracks in a surface coating layered material under thermal stresses due to rolling/sliding contact with heat input. Contact loading is simulated as a contact pressure load with both the normal and shear components having parabolic distribution. Attention here is focused on the energy release rate at the crack tips which provide a measure for quantifying the magnitude of interface crack growth. In the present crack analysis, the interface cracks are replaced by the distributed edge dislocations, and the crack face friction is negrected. The problem is reduced to simultaneous singular integral equations for dislocation densities. The integral equations can be solved numerically by considering the nature of the singularities at the crack tips. The numerical results of the energy release rate showing the effects of the mutual interference of a pair of interface cracks are given for some tribological material coatings on a steel substrate. The effects of the frictional coefficient, the heat input strength and the coating thickness upon the magnitude of the energy release rate and it's mutual interference are considered numerically.

Key Words: Elasticity, Thermal Stress, Rolling-Sliding Contact, Interface Crack, Multiple Cracks, Mutual Interference, Energy Release Rate, Coating Layered Material

1. Introduction

The surface coating materials are more and more used to improve the mechanical and tribological behavior of surfaces in the industries. In most cases, rolling contacts are accompanied by heat generation such as an excessive frictional heating caused by its relative slip between the two sliding surfaces. In a hot rolling process, in addition to the frictional heat generation, the work roll is subjected to a great deal of heat input in the contact region by heat transfer from a hot strip. Then, thermomechanical cracking can be occur on the interface of these coating materials when they are subjected to the rolling/sliding contact. In recent years, a considerable effort has been devoted to thermomechanical contact problem in the layered materials. Ju and coworkers[1]-[3] analyzed the thermoelastic contact problem in the various layered half-space due to a moving heat source and a moving mechanical load of combined pressure and tangential friction. Leory et al.[4] analyzed the thermal stresses in the multilayered media due to a moving heat source. Chen et al.[5] analyzed the transient thermal stresses due to periodic moving frictional load in the layered half-space. Although these studies for thermomechanical contact problem are useful to gain a basic understanding for the stress field in tribology, they do not involved in the crack analysis. In order to gain a better understanding for the conditions of fracture in tribology, it is nessary to solve the thermomechanical crack problems by means of the fracture mechanics. Recently, one of the authors[6],[7] has dealt with the thermomechanical crack problems for the surface layered materials due to the rolling contact with heat

* Received 31st March, 1999
** Faculty of Engineering, Toyama University, 3190 Gofuku, Toyama City 930-8555, Japan. E-mail: goshima@eng.toyama-u.ac.jp
*** Faculty of Science and Engineering, Chuo University, 1-13-27 Kasuga, Bunkyo-ku, Tokyo 112-0003, Japan

input such as a frictional heating. These studies deal with a single finite crack problem, and do not involve in the multiple interface crack analysis. However, in the many actual thermomechanical rolling contact problem, the multiple interface cracks will happen to be initiated and propagate with high growth rate due to the mutual interference between the multiple cracks. Therefore, in order to gain a better understanding for the conditions of fracture with debonding in layered materials due to rolling contact, thermomechanical effects and the mutual interference effects of these multiple interface cracks due to rolling contact must be considered.

In this study, we deal with the two-dimensional multiple interface crack problem for a surface coating layered material under thermal stresses due to rolling/sliding contact with heat input. Contact loading is simulated as a contact pressure load with both the normal and shear components having parabolic distribution. In the present crack analysis, the interface cracks are replaced by the distributed edge dislocations, and the crack face friction is neglected. In the temperature analysis, the speed of the moving contact region is assumed to be much greater than the ratio of the thermal diffusivity and the contact length (large Peclet number), and that the temperature distribution is not disturbed by these cracks. The problem is reduced to simultaneous singular integral equations for dislocation densities. The integral equations can be solved numerically by considering the nature of the singularities at the crack tips. The solution of dislocation densities directly deduce the complex stress intensity factors. Accordingly, the energy release rates are also obtained. It was found that the total strain energy release rate remained relatively constant as the crack propagated along the interface[8]. Moreover, the total energy release rate approach eliminated the problems associated with the oscillating singularities. In fact, the total energy release rate has been used frequently as a fracture parameter for interfacial crack propagation. Therefore, attention here is focused on the energy release rate at the crack tips which provide a measure for quantifying the magnitude of interface crack growth. The numerical results of the energy release rate showing the effects of the mutual interference of a pair of interface cracks are given for some tribological material coatings on a steel substrate. The effects of the frictional coefficient, the amount of the heat input and the coating thickness upon the magnitude of the energy release rate and it's mutual interference with the distance between a pair of interface cracks are considered numerically.

2. Problem Formulation

An elastic surface layered half-space containing multiple interface cracks is subjected to rolling-sliding contact accompanied by heat input with constant moving velocity V as shown in Fig. 1. The surface of the layered half-space is loaded by an arbitrarily distributed contact pressure $P_1(\tilde{x})$ and tangential frictional load $fP_1(\tilde{x})$ in the contact region (where f is frictional coefficient). Then, the heat generation $Q_1(\tilde{x})$ in the contact region is given as the sum of a frictional heat generation $fV_sP_1(\tilde{x})$ and a heat input $Q_0(\tilde{x})$ as follows:

$$Q_1(\tilde{x})=fV_sP_1(\tilde{x})+Q_0(\tilde{x})=fS_rVP_0P(x)+q_0Q(x) \quad (1)$$

where, V_s is the sliding velocity during rolling contact. In the present analysis, the following dimensionless parameter are used.

$$(x, y)=(\tilde{x}/c, \tilde{y}/c),\ (x_k, y_k)=(\tilde{x}_k/c, \tilde{y}_k/c),$$
$$l_k=\tilde{l}_k/c,\ d=\tilde{d}/c,\ h=\tilde{h}/c,\ e_k=\tilde{e}_k/c,$$
$$d^*=\tilde{d}_{k-1}/c-(l_1+l_k),\ R_g=cV/k_g,\ S_r=V_s/V,$$
$$\lambda=q_0/P_0V,\ K=K_2/K_1,\ G_{12}=G_2/G_1,$$
$$\alpha_{12}=\alpha_2/\alpha_1,\ \nu_{21}=(1-\nu_1)/(1-\nu_2),$$
$$\nu_{12}=(1+\nu_2)/(1+\nu_1),\ P(x)=P_1(\tilde{x})/P_0,$$
$$Q(x)=Q_0(\tilde{x})/q_0,\ H_1=E_1\alpha_1k_1/\{K_1(1-\nu_1)\},$$
$$\alpha=\frac{G_2(\kappa_1+1)-G_1(\kappa_2+1)}{G_2(\kappa_1+1)+G_1(\kappa_2+1)},$$
$$\beta=\frac{G_2(\kappa_1-1)-G_1(\kappa_2-1)}{G_2(\kappa_1+1)+G_1(\kappa_2+1)},$$
$$C=\frac{2G_1(1+\alpha)}{(\kappa_1+1)(1-\beta^2)}=\frac{2G_2(1-\alpha)}{(\kappa_2+1)(1-\beta^2)},$$
$$T^*=cVP_0/K_1 \quad (2)$$

where, k_g is thermal diffusivity, K_g is thermal conductivity, P_0 is the maximum contact pressure and q_0 is the maximum heat input, G_g is shear modulus, ν_g is the Poisson's ratio, α_g is coefficient of thermal expansion, E_g is Young's modulus, R_g is Peclet number, S_r is slide/roll ratio, λ is the dimensionless parameter which represents the heat input strength. α, β are the Dundurs' parameters being $\kappa_g=3-4\nu_g$ for plane strain, $\kappa_g=(3-\nu_g)/(1+\nu_g)$ for plane stress. The sub-

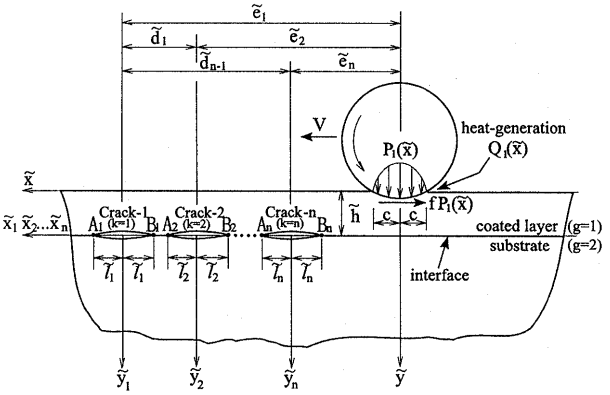

Fig. 1 Problem configuration and coordinate systems

script $g=1$ and $g=2$ denote coated layer and substrate regions respectively. The parameters for the crack-k are represented by the subscript k (where $k=1, 2, \cdots, n$).

The region outside the area of contact is assumed to be thermally insulated. Furthermore, it is assumed that the temperature distribution is not affected by the presence of cracks. The thermal boundary conditions can now be given as follows.

$$\frac{\partial T^{(1)}}{\partial y}=\begin{cases}-T^*\{fS_rP(x)+\lambda Q(x)\}, & |x|\leq 1,\ y=0\\ 0, & |x|>1,\ y=0\end{cases} \quad (3)$$

$$\frac{\partial T^{(1)}}{\partial y}=K\frac{\partial T^{(1)}}{\partial y},\ y=h \quad (4)$$

$$T^{(1)}=T^{(2)},\ y=h \quad (5)$$

$$T^{(g)}=0,\ (g=1, 2),\ x^2+y^2\to\infty \quad (6)$$

The mechanical boundary conditions on the surface, interface and at infinity of the half-space are given as follows.

$$\sigma_{yy}^{(1)}=\begin{cases}-P_0P(x), & |x|\leq 1,\ y=0\\ 0, & |x|>1,\ y=0\end{cases} \quad (7)$$

$$\sigma_{xy}^{(1)}=\begin{cases}fP_0P(x), & |x|\leq 1,\ y=0\\ 0, & |x|>1,\ y=0\end{cases} \quad (8)$$

$$\sigma_{yy}^{(1)}=\sigma_{yy}^{(2)},\ y=h \quad (9)$$

$$\sigma_{xy}^{(1)}=\sigma_{xy}^{(2)},\ y=h \quad (10)$$

$$U_{xx}^{(1)}=U_{xx}^{(2)},\ y=h \quad (11)$$

$$U_{yy}^{(1)}=U_{yy}^{(2)},\ y=h \quad (12)$$

$$\sigma_{pq}^{(g)}=0,\ (p, q=x, y),\ (g=1, 2, \cdots, n),\ x^2+y^2\to\infty \quad (13)$$

Assuming that the crack face friction is neglected, the boundary conditions along the cracks may be expressed as follows.

$$\sigma_{y_ky_k}^{(g)}=0,\ (g=1, 2, \cdots, n),\ x_k\in x_k^{op},\ y_k=0,\ (k=1, 2, \cdots, n) \quad (14)$$

$$\sigma_{x_ky_k}^{(g)}=0,\ (g=1, 2, \cdots, n),\ -l_k\leq x\leq l_k,\ y_k=0,\ (k=1, 2, \cdots, n) \quad (15)$$

$$U_{y_ky_k}^{(1)}=U_{y_ky_k}^{(2)},\ x_k\in x_k^{cl},\ y_k=0,\ (k=1, 2, \cdots, n) \quad (16)$$

where x_k^{op} and x_k^{cl} are the crack face opening and closing region, respectively.

3. Stress Analysis

3.1 Temperature analysis

The quasi-stationary temperature solution in a layered half-space due to fast-moving heat source, which satisfies the boundary conditions Eqs. (3)-(6), is given in the Fourier transformed space as follows[1].

$$\bar{T}^{(g)}=T^*\{fS_r\bar{P}(s)+\lambda\bar{Q}(s)\}F^{(g)}(s)/D_s,\ (g=1, 2) \quad (17)$$

where,

$$F^{(1)}(s)=\cosh\{(h-y)\beta_1\}+K\beta_{12}\sinh\{(h-y)\beta_1\},$$

$$F^{(2)}(s)=\exp\{(h-y)\beta_2\},$$

$$D_s=\beta_1\sinh(h\beta_1)+K\beta_2\cosh(h\beta_1),$$

$$\beta_{12}=\beta_2/\beta_1,\ \beta_g=(isR_g)^{1/2},\ i=\sqrt{-1}$$

and $\bar{T}^{(g)}$ is the Fourier transform of the temperature $T^{(g)}$ defined as follows.

$$\bar{T}^{(g)}=(2\pi)^{-1/2}\int_{-\infty}^{\infty}T^{(g)}\exp(isx)dx,\ (g=1, 2) \quad (18)$$

Then, the inverse transform is given by the following complex integration as:

$$T^{(g)}=(2\pi)^{-1/2}\int_{-\infty}^{\infty}\bar{T}^{(g)}\exp(-isx)ds,\ (g=1, 2) \quad (19)$$

here, "s" denotes the complex parameter.

3.2 Superposition method for stress analysis

The stress field $\sigma_{pq}^{(g)}$ in the cracked layered half-space subjected to rolling-sliding contact and heat input is represented by superposition as:

$$\sigma_{pq}^{(g)}={}^0\sigma_{pq}^{(g)}+{}^1\sigma_{pq}^{(g)},\ (p, q=x, y),\ (g=1, 2) \quad (20)$$

here, ${}^0\sigma_{pq}^{(g)}$ denote the thermal stresses in an uncracked layered half-space subjected to rolling-sliding contact and heat input. The stresses ${}^1\sigma_{pq}^{(g)}$ denotes the disturbance by the multiple cracks, which satisfy the continuity conditions at the interface along with the stress free conditions on the surface.

3.3 Thermal stresses in an uncracked layered media

The thermal stresses ${}^0\bar{\sigma}_{pq}^{(g)}$ due to the temperature field Eq. (17) can be expressed in the Fourier transformed space as follows.

$$\frac{{}^0\bar{\sigma}_{xx}^{(g)}}{2G_g}=-s^2\bar{\Phi}_0^{(g)}-s^2y\bar{\Phi}_3^{(g)}-2\nu_g\frac{\partial\bar{\Phi}_3^{(g)}}{\partial y}-\frac{\partial^2\bar{\Omega}^{(g)}}{\partial y^2}$$

$$\frac{{}^0\bar{\sigma}_{yy}^{(g)}}{2G_g}=\frac{\partial^2\bar{\Phi}_0^{(g)}}{\partial y^2}+y\frac{\partial^2\bar{\Phi}_3^{(g)}}{\partial y^2}-2(1-\nu_g)\frac{\partial\bar{\Phi}_3^{(g)}}{\partial y}+s^2\bar{\Omega}^{(g)}$$

$$\frac{{}^0\bar{\sigma}_{xy}^{(g)}}{2G_g}=-is\left\{\frac{\partial\bar{\Phi}_0^{(g)}}{\partial y}+y\frac{\partial\bar{\Phi}_3^{(g)}}{\partial y}-(1-2\nu_g)\bar{\Phi}_3^{(g)}+\frac{\partial\Omega^{(g)}}{\partial y}\right\},\ (g=1, 2) \quad (21)$$

Where, the thermoelastic potential $\bar{\Omega}^{(g)}$ and the stress functions $\bar{\Phi}_r^{(g)}$ $(r=0, 3)$ in the Fourier transformed space are given as:

$$\bar{\Omega}^{(g)}=\frac{1+\nu_g}{1-\nu_g}\alpha_g\frac{\bar{T}^{(g)}}{\beta_g^2-s^2},\ (g=1, 2) \quad (22)$$

$$\bar{\Phi}_r^{(g)}=C_r^{(g)}\exp(-sy)+D_r^{(g)}\exp\{-s(h-y)\},\ (g=1, 2:\ r=0, 3) \quad (23)$$

here, $C_r^{(g)}, D_r^{(g)}$ $(g=1, 2:\ r=0, 3)$ are the unknown constants. By applying the boundary conditions Eqs. (7)-(13), the coefficients $C_r^{(g)}, D_r^{(g)}$ can be solved from algebraic equations. Consequently, the thermal stresses ${}^0\bar{\sigma}_{pq}^{(g)}$ are obtained in the Fourier transformed space as follows.

$$\begin{aligned}{}^0\bar{\sigma}_{xx}^{(1)}/P_0=&-s^2C_0^{(1)}\exp(-sy)\\&-s^2D_0^{(1)}\exp\{-s(h-y)\}\\&-(s^2y-2s\nu_1)C_3^{(1)}\exp(-sy)\\&-(s^2y+2s\nu_1)D_3^{(1)}\exp\{-s(h-y)\}\\&-H_1R_1\{fS_r\bar{P}(s)+\lambda\bar{Q}(s)\}\beta_1^2F_{(s)}^{(1)}/(\beta_1^2-s^2)\end{aligned} \quad (24)$$

$$\begin{aligned}{}^0\bar{\sigma}_{yy}^{(1)}/P_0=&s^2C_0^{(1)}\exp(-sy)\\&+s^2D_0^{(1)}\exp\{-s(h-y)\}\\&+\{s^2y-2s(1-\nu_1)\}C_3^{(1)}\exp(-sy)\end{aligned}$$

$$+(s^2y-2s(1-\nu_1))D_3^{(1)}\exp\{-s(h-y)\}$$
$$+H_1R_1\{fS_r\bar{P}(s)+\lambda\bar{Q}(s)\}s^2F_{(s)}^{(1)}/(\beta_1^2-s^2) \quad (25)$$

$${}^0\bar{\sigma}_{xy}^{(1)}/P_0=is[sC_0^{(1)}\exp(-sy)$$
$$-sD_0^{(1)}\exp\{-s(h-y)\}$$
$$+(sy+1-2\nu_1)C_3^{(1)}\exp(-sy)$$
$$-(sy-1+2\nu_1)D_3^{(1)}\exp\{-s(h-y)\}$$
$$+H_1R_1\{fS_r\bar{P}(s)+\lambda\bar{Q}(s)\}\beta_1F_{(s)}^{(1)}/(\beta_1^2-s^2)] \quad (26)$$

$${}^0\bar{\sigma}_{xx}^{(2)}/P_0=G[-s^2C_0^{(2)}\exp\{-s(y-h)\}$$
$$-s^2yC_3^{(2)}\exp\{-s(y-h)\}$$
$$+2s\nu_2C_3^{(2)}\exp\{-s(y-h)\}$$
$$-H_1R_1\{fS_r\bar{P}(s)+\lambda\bar{Q}(s)\}\nu_{21}\nu_{12}\alpha\beta_2^2F_{(s)}^{(2)}$$
$$/(\beta_2^2-s^2)] \quad (27)$$

$${}^0\bar{\sigma}_{yy}^{(2)}/P_0=G[s^2C_0^{(2)}\exp\{-s(y-h)\}$$
$$+s^2yC_3^{(2)}\exp\{-s(y-h)\}$$
$$+2s(1-\nu_2)C_3^{(2)}\exp\{-s(y-h)\}$$
$$+H_1R_1\{fS_r\bar{P}(s)+\lambda\bar{Q}(s)\}\nu_{21}\nu_{12}\alpha s^2F_{(s)}^{(2)}$$
$$/(\beta_2^2-s^2)] \quad (28)$$

$${}^0\bar{\sigma}_{xy}^{(2)}/P_0=isG[sC_0^{(2)}\exp\{-s(y-h)\}$$
$$+syC_3^{(2)}\exp\{-s(y-h)\}$$
$$+(1-2\nu_2)C_3^{(2)}\exp\{-s(y-h)\}$$
$$+H_1R_1\{fS_r\bar{P}(s)+\lambda\bar{Q}(s)\}\nu_{21}\nu_{12}\alpha\beta_2F_{(s)}^{(2)}$$
$$/(\beta_2^2-s^2)] \quad (29)$$

The inverse Fourier transform of Eqs.(24)-(29) are given by carrying out the complex integration as:

$${}^0\sigma_{pq}^{(g)}=(2\pi)^{-1/2}\int_{-\infty}^{\infty}{}^0\bar{\sigma}_{pq}^{(g)}\exp(-isx)ds,$$
$$(p, q=xy),\ (g=1, 2) \quad (30)$$

Since the general solutions of the above complex integration Eqs.(19) and (30) are too complicated to invert analytically, in the present study, we use the numerical integration technique which is analogous to that used by Ju, et al.[9] in order to avoid the singularity at $s=0$ and $s=iR_g$. Thus, we can obtain the thermal stress solution ${}^0\sigma_{pq}^{(g)}$ in an uncracked layered media, which satisfy the boundary conditions Eqs. (7)-(13).

3.4 Stress field due to the multiple interface cracks

To account for the disturbance ${}^1\sigma_{pq}^{(g)}$ by the multiple cracks, which satisfy the continuity conditions at the interface along with the stress free conditions on the surface, we consider the problem of a discrete edge dislocation (b_{x_k}, b_{y_k}) located at $(\eta_k, 0)$ in the coordinate system (x_k, y_k) being at the interface of two bonded dissimilar half-space as shown in Fig. 2. The edge dislocation (b_{x_k}, b_{y_k}) are shown as:

$$b_{x_k}=[U_{x_kx_k}]/c,\ b_{y_k}=[U_{y_ky_k}]/c,\ (k=1, 2, \cdots, n) \quad (31)$$

where, $[U_{x_kx_k}], [U_{y_ky_k}]$ represent the displacement jumps. This stress solution, ${}^x\sigma_{pq}^{(g)}(x_k, y_k)$ and ${}^y\sigma_{pq}^{(g)}(x_k, y_k)$; $(p, q=x_k, y_k)$ due to b_{x_k} and b_{y_k} respectively, have been analyzed by Dundurs[10]. For example, the stresses at the interface are shown as:

$${}^x\sigma_{y_ky_k}(x_k, 0)=-\beta Cb_{x_k}\delta(x_k-\eta_k) \quad (32)$$

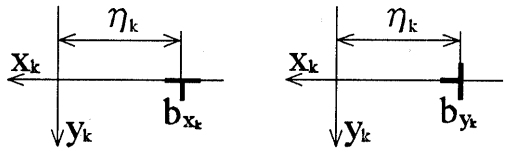

Fig. 2 Geometry for the glid and climb dislocations (b_{x_k} and b_{y_k}) located at the interface

$${}^x\sigma_{x_ky_k}(x_k, 0)=\frac{Cb_{x_k}}{\pi}\frac{1}{(x_k-\eta_k)} \quad (33)$$

$${}^y\sigma_{y_ky_k}(x_k, 0)=\frac{Cb_{y_k}}{\pi}\frac{1}{(x_k-\eta_k)} \quad (34)$$

$${}^y\sigma_{x_ky_k}(x_k, 0)=\beta Cb_{y_k}\delta(x_k-\eta_k) \quad (35)$$

where, $\delta(x_k)$ is the Dirac's delta function.

Although the stress fields ${}^x\sigma_{pq}^{(g)}(x_k, y_k)$, ${}^y\sigma_{pq}^{(g)}(x_k, y_k)$ satisfy the continuity conditions at the interface, the stress free conditions on the layered surface is not satisfied. Therefore, in order to remove the surface tractions and satisfy the stress free conditions on the layered surface, the additional stresses ${}^A\sigma_{pq}^{(g)}$, ${}^B\sigma_{pq}^{(g)}$ must be considered as follows.

$${}^{bx}\sigma_{pq}^{(g)}={}^x\sigma_{pq}^{(g)}+{}^A\sigma_{pq}^{(g)},\ (p, q=x_k, y_k,\ g=1, 2) \quad (36)$$

$${}^{by}\sigma_{pq}^{(g)}={}^y\sigma_{pq}^{(g)}+{}^B\sigma_{pq}^{(g)},\ (p, q=x_k, y_k,\ g=1, 2) \quad (37)$$

The complimentary stresses ${}^A\sigma_{pq}^{(g)}$, ${}^B\sigma_{pq}^{(g)}$ can be obtained in the same manner as Eqs.(21)-(30) with $\bar{Q}^{(g)}=0$. The unknown constants being equivalent to $C_r^{(g)}$, $D_r^{(g)}$ in Eq.(23) can be determined by solving algebraic equations to meet the stress free conditions on the layered surface along with the continuity conditions at the interface.

Replacing b_{x_k} and b_{y_k} by distributed dislocation density $b_{x_k}d\eta_k$ and $b_{y_k}d\eta_k$ defined along the line of the crack-k, the stresses ${}^1\sigma_{pq,k}^{(g)}$ induced by the crack-k can be obtained by integration of η_k as follows.

$${}^1\sigma_{pq,k}^{(g)}=\int_{-l_k}^{l_k}({}^{bx}\sigma_{pq}^{(g)}+{}^{by}\sigma_{pq}^{(g)})d\eta_k,$$
$$(p, q=x_k, y_k),\ (g=1, 2) \quad (38)$$

Therefore, the stress disturbance ${}^1\sigma_{pq}^{(g)}$ by the multiple cracks $(k=1, 2, \cdots, n)$, which satisfy the continuity conditions at the interface along with the stress free conditions on the surface, can be obtained by superposing the stresses ${}^1\sigma_{pq,k}^{(g)}$ $(k=1, 2, \cdots, n)$ as follows.

$${}^1\sigma_{pq}^{(g)}=\sum_{k=1}^{n}{}^1\sigma_{pq,k}^{(g)},\ (p, q=x_k, y_k,\ g=1, 2) \quad (39)$$

4. Stress Intensity Factors and Energy Release Rate

4.1 Derivation of the integral equations by the crack face boundary conditions

Substitution of Eq.(30), (39) into Eq.(20) and the remaining boundary condition along the multiple cracks Eqs.(14), (15) leads directly to the following simultaneous singular integral equations for $B_{x_k}(x_k)$,

$B_{y_k}(x_k)$ $(k=1, 2, \cdots, n)$.

$$\frac{C}{\pi}\int_{-l_j}^{l_j}\frac{B_{y_j}(\eta_j)}{G_1(x_j-\eta_j)}d\eta_j-\beta\frac{C}{G_1}B_{x_j}(x_j)+\sum_{k=1}^{n}\left\{\int_{-l_k}^{l_k}2B_{x_k}(\eta_k)\Gamma_{1k}(x_k,\eta_k)d\eta_k+\int_{-l_k}^{l_k}2B_{y_k}(\eta_k)\Gamma_{2kj}(x_k,\eta_k)d\eta_k\right\}=-\frac{{}^0\sigma_{y_jy_j}^{(1)}}{P_0}$$
$$x_j\in x_j^{op},\ y_j=0,\ (j=1, 2, \cdots, n) \tag{40}$$

$$\frac{C}{\pi}\int_{-l_j}^{l_j}\frac{B_{y_j}(\eta_j)}{G_1(x_j-\eta_j)}d\eta_j+\beta\frac{C}{G_1}B_{y_j}(x_j)+\sum_{k=1}^{n}\left\{\int_{-l_k}^{l_k}2B_{x_k}(\eta_k)\Gamma_{3kj}(x_k,\eta_k)d\eta_k+\int_{-l_k}^{l_k}2B_{y_k}(\eta_k)\Gamma_{4k}(x_k,\eta_k)d\eta_k\right\}=-\frac{{}^0\sigma_{x_jy_j}^{(1)}}{P_0}$$
$$-l_j\le x_j\le l_j,\ y_j=0,\ (j=1, 2, \cdots, n) \tag{41}$$

where,

$$B_{x_k}(x_k)=\frac{G_1b_{x_k}}{P_0},\ G_{y_k}(x_k)=\frac{G_1b_{y_k}}{P_0},\quad (k=1, 2, \cdots, n) \tag{42}$$

$$\Gamma_{1k}(x_k,\eta_k)=\int_0^\infty\left\{\left(\alpha_1^{(1)}-\frac{\kappa_1+1}{2}\beta_1^{(1)}\right)+\left(\alpha_2^{(1)}+\frac{\kappa_1+1}{2}\beta_2^{(1)}\right)e^{-h\xi_k}\right\}\cos\{\xi_k(x_k-\eta_k)\}d\xi_k \quad (k=1, 2, \cdots, n) \tag{43}$$

$$\Gamma_{2kj}(x_k,\eta_k)=\int_0^\infty\left\{\left(\gamma_1^{(1)}-\frac{\kappa_1+1}{2}\varepsilon_1^{(1)}\right)+\left(\gamma_2^{(1)}+\frac{\kappa_1+1}{2}\varepsilon_2^{(1)}\right)e^{-h\xi_k}\right\}\sin\{\xi_k(x_k-\eta_k)\}d\xi_k+(1-\delta_{kj})\frac{C}{2\pi G_1(x_k-\eta_k)} \quad (k=1, 2, \cdots, n),\ (j=1, 2, \cdots, n) \tag{44}$$

$$\Gamma_{3kj}(x_k,\eta_k)=\int_0^\infty\left\{\left(-\alpha_1^{(1)}+\frac{\kappa_1-1}{2}\beta_1^{(1)}\right)+\left(\alpha_2^{(1)}+\frac{\kappa_1-1}{2}\beta_2^{(1)}\right)e^{-h\xi_k}\right\}\sin\{\xi_k(x_k-\eta_k)\}d\xi_k+(1-\delta_{kj})\frac{C}{2\pi G_1(x_k-\eta_k)} \quad (k=1, 2, \cdots, n),\ (j=1, 2, \cdots, n) \tag{45}$$

$$\Gamma_{4k}(x_k,\eta_k)=\int_0^\infty\left\{\left(\gamma_1^{(1)}-\frac{\kappa_1-1}{2}\varepsilon_1^{(1)}\right)-\left(\gamma_2^{(1)}+\frac{\kappa_1-1}{2}\varepsilon_2^{(1)}\right)e^{-h\xi_k}\right\}\cos\{\xi_k(x_k-\eta_k)\}d\xi_k \quad (k=1, 2, \cdots, n) \tag{46}$$

$$\delta_{kj}=\begin{cases}1 & k=j\\ 0 & k\neq j\end{cases}$$

Here, $\alpha_1^{(1)}$, $\alpha_2^{(1)}$, $\beta_1^{(1)}$, $\beta_2^{(1)}$, $\gamma_1^{(1)}$, $\gamma_2^{(1)}$, $\varepsilon_1^{(1)}$, $\varepsilon_2^{(1)}$ are the constants which have been obtained by solving algebraic equations to meet the boundary conditions on the layered surface along with the continuity conditions at the interface.

We must require in addition that the total Burgers vectors of the dislocations along each cracks vanish, or that

$$\int_{-l_k}^{l_k}B_{x_k}(\eta_k)d\eta_k=0,\ \int_{-l_k}^{l_k}B_{y_k}(\eta_k)d\eta_k=0,\quad (k=1, 2, \cdots, n) \tag{47}$$

as the conditions ensure that the displacements are single-valued.

4. 2 Numerical calculations of integral equations and energy release rate

The simultaneous singular integral equation given by Eqs.(40)-(47) was solved numerically. Replacing the parameter η_k, $x_k[-l_k, l_k]$ by $\hat{\eta}_k$, $\hat{x}_k[-1, 1]$ as:

$$\hat{\eta}_k=\frac{\eta_k}{l_k},\ \hat{x}_k=\frac{x_k}{l_k},\ (k=1, 2, \cdots, n) \tag{48}$$

the dimensionless dislocation density $B_{x_k}(\hat{\eta}_k)$, $B_{y_k}(\hat{\eta}_k)$ can be written as follows.

$$B_m(\zeta)=\frac{g_m(\zeta)}{(1-\zeta)^\gamma(1+\zeta)^\delta},\ (m=x_k, y_k),\quad (\zeta=\hat{\eta}_k,\ \hat{x}_k)\ (k=1, 2, \cdots, n) \tag{49}$$

$$\gamma=\frac{1}{2}+i\omega,\ \delta=\frac{1}{2}-i\omega,\ \omega=\frac{1}{2\pi}\ln\left(\frac{1+\beta}{1-\beta}\right) \tag{50}$$

Substituting Eq.(49) into Eqs.(40), (41) and (47), and using the technique developed by Miller and Keer[11], the integral equation Eqs.(40)-(47) reduce to the simultaneous algebraic equations for $g_m(\zeta)$. In solving these equations, the crack face opening region x_k^{op} or closing region x_k^{cl} for each cracks $(k=1, 2, \cdots, n)$ are determined by the iteration method under the condition of absence of overlap of the materials at the each interface crack faces. The boundary condition Eq. (16) can be satisfied by setting $g_{y_k}(\zeta)=0$ for the portion of $x\in x_k^{cl}$.

Then, the complex stress intensity factors can be determined as follows.

$$\frac{K_{A_k}}{P_0\sqrt{c}}=\frac{K_1^{A_k}+iK_2^{A_k}}{P_0\sqrt{c}}=\frac{\sqrt{\pi l_k}(2l_k)^{i\omega}C}{G_1}\times\sqrt{1-\beta^2}\{g_{y_k}(1)+ig_{x_k}(1)\},$$
at the crack tips A_K $(k=1, 2, \cdots, n)$ (51)

$$\frac{K_{B_k}}{P_0\sqrt{c}}=\frac{K_1^{B_k}+iK_2^{B_k}}{P_0\sqrt{c}}=-\frac{\sqrt{\pi l_k}(2l_k)^{i\omega}C}{G_1}\times\sqrt{1-\beta^2}\{g_{y_k}(-1)+ig_{x_k}(-1)\},$$
at the crack tips B_k $(k=1, 2, \cdots, n)$ (52)

whereas, the energy release rates for each crack tips are given as follows[12),(13)].

$$G_{A_k}^*=\frac{G_1}{P_0^2C}G_{A_k}=\frac{K_{A_k}^*\bar{K}_{A_k}^*}{16}\sqrt{1-\beta^2}\{\kappa_1+1+(\kappa_2+1)G_{12}\}$$
at the crack tips A_k $(k=1, 2, \cdots, n)$ (53)

$$G_{B_k}^*=\frac{G_1}{P_0^2C}G_{B_k}=\frac{K_{B_k}^*\bar{K}_{B_k}^*}{16}\sqrt{1-\beta^2}\{\kappa_1+1+(\kappa_2+1)G_{12}\}$$
at the crack tips B_k $(k=1, 2, \cdots, n)$ (54)

where,

$$K_{A_k}^*=K_{A_k}/P_0\sqrt{c},\ K_{B_k}^*=K_{B_k}/P_0\sqrt{c} \tag{55}$$

5. Numerical Results of Energy Release Rate

Numerical calculations were carried out for the case of a couple of interface cracks $(k=2)$ with equal length $(2l_1=2l_2=0.1)$. As the actual coating examples, three kinds of tribological coating materials bonded to the carbon steel substrate are considered. They are

Table 1 Material properties

	Layer(g=1) (Al_2O_3)	Layer(g=1) (SiC)	Layer(g=1) (Stellite)	Substrate(g=2) (Carbon Steel)
E_g (GPa)	390.0	320.0	240.0	207.0
ν_g	0.23	0.127	0.285	0.3
G_g (GPa)	158.5	142.0	93.4	79.6
K_g (W/mK)	20.73	104.4	9.7	36.053
k_g (m^2/s)	4.99×10^{-6}	49.0×10^{-6}	2.77×10^{-6}	9.72×10^{-6}
α_g (K^{-1})	7.19×10^{-6}	5.01×10^{-6}	11.3×10^{-6}	10.0×10^{-6}
β	-0.05927	0.007648	-0.01281	

Aluminum Oxide (Al_2O_3), Silicon Carbon (SiC) and Stellite III (St). These material properties are shown in Table 1. The contact pressure $P(x)$ in Eqs.(3), (7), (8) and the heat input distribution $Q(x)$ in Eq. (3) were both assumed to have parabolic distributions. The Peclet number was taken as $R_1=200.4(Al_2O_3)$, $R_1=20.4(SiC)$, $R_1=361.0(St)$, $R_1=102.9$(Carbon steel), being $cV=1.0\times10^{-3}\,m^2/s$. The slide/roll ratio was assumed to be taken as $S_r=0.1$. All of the following results are shown as the dimensionless energy release rate G^*_{Ak}, G^*_{Bk} $(k=1,2)$ being defined in Eqs.(53), (54).

The numerical results of the energy release rates $G^*_{A_1}$, $G^*_{A_2}$ of each crack tips (A_1, A_2) are plotted as functions of the crack location over a complete loading cycle in Figs. 3 and 4 for $\lambda=0$ (no heat input) and $\lambda=1.5$, respectively. All these results are shown for the case of $h=0.1$ and $d^*=0.01$. Although, in the present numerical examples, these results are shown only at the crack tips A_1, A_2, the results of the energy release rates at the crack tips B_1, B_2 are almost equal to the results at A_1, $A_2(G^*_{A_1}\cong G^*_{B_2},\ G^*_{A_2}\cong G^*_{B_1})$. From these figures, we can see that the magnitude of all the results of $G^*_{A_2}$ at the inside tip of crack-2 are always greater than that of $G^*_{A_1}$ at the outside tip of crack-1, regardless of the kinds of coating materials, the frictional coefficient f and the strength of heat input λ. From Fig. 3 (no heat-input: $\lambda=0$), for the case of the small frictional coefficient ($f=0.1$), $G^*_{A_1}$, $G^*_{A_2}$ show the maximum values at about $x=-0.8$ which corresponds to the cracks being under the vicinity of the right edge of the contact region. While, for the case of large frictional coefficient ($f=0.7$), the crack location which maximize $G^*_{A_1}$, $G^*_{A_2}$ approach to $x=0$ which corresponds to the cracks being under the center of the contact region. The value of $G^*_{A_1}$, $G^*_{A_2}$ increase with an increase of frictional coefficient. Especially, this tendency are remarkable for the case of SiC-coating. For the case of large heat-input $\lambda=1.5$ (in Fig. 4), the magnitude of $G^*_{A_1}$, $G^*_{A_2}$ tremendously increase compared to those in Fig. 3. Especially, this tendency are remarkable for the case of Stellite-coating. The

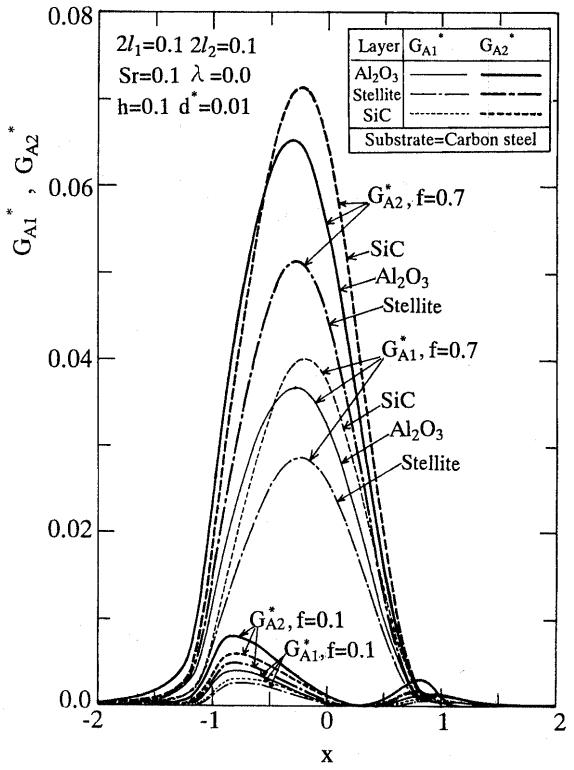

Fig. 3 Energy release rates at the both tips of crack-1 and crack-2 as functions of crack location for $f=0.1$ and 0.7 being $\lambda=0.0$

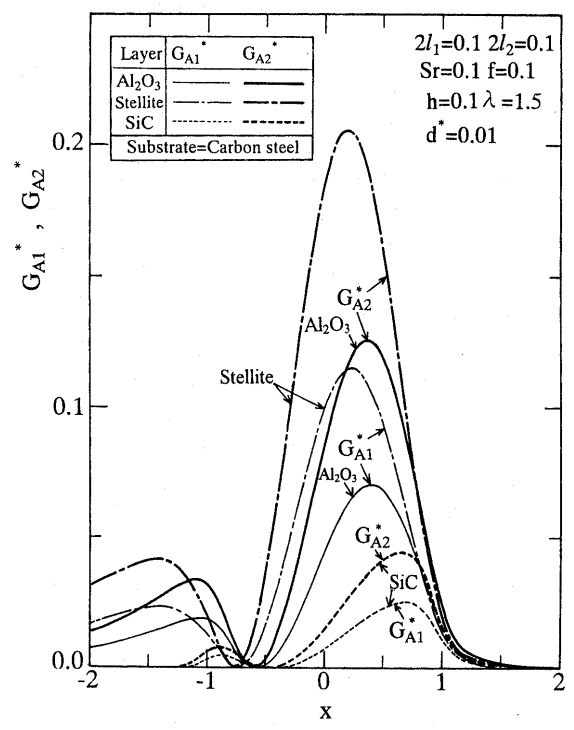

Fig. 4 Energy release rates at the both tips of crack-1 and crack-2 as functions of crack location for $\lambda=1.5$ being $f=0.1$

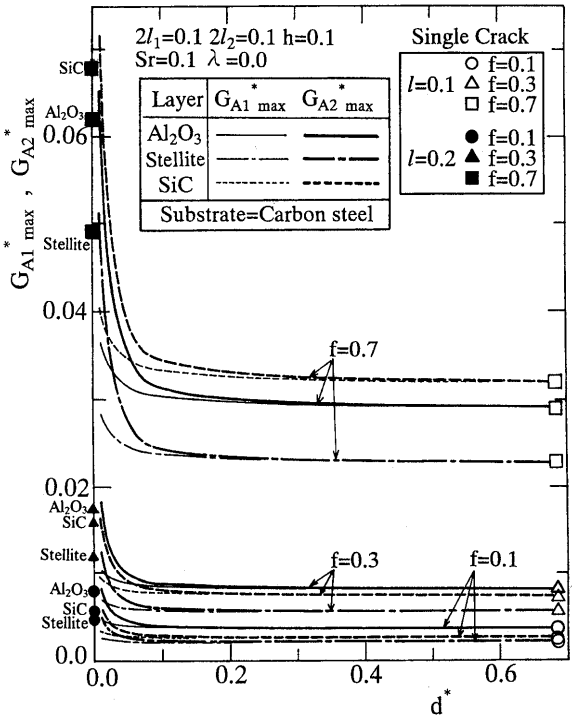

Fig. 5 Interference effects on the maximum energy release rate with a decrease of the distance between the two cracks for the various values of frictional coefficients $f=0.1$, 0.3 and 0.7

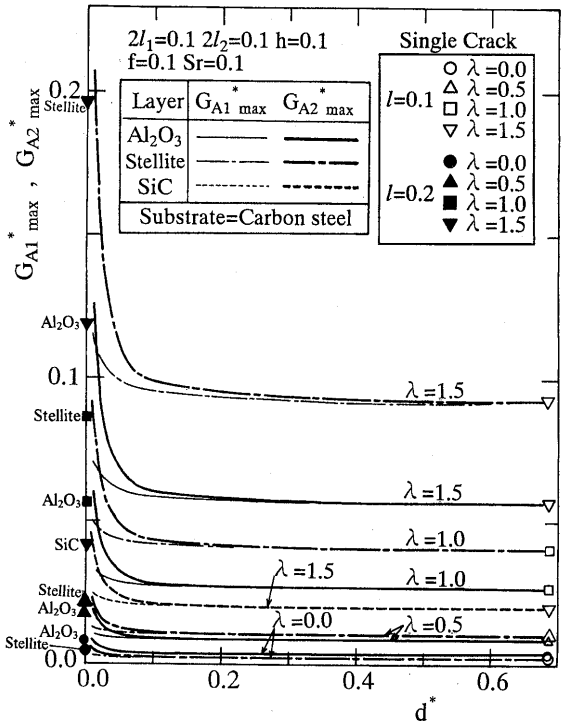

Fig. 6 Interference effects on the maximum energy release rate with a decrease of the distance between the two cracks for the various values of heat input parameter $\lambda=0.0$, 0.5, 1.0 and 1.5

crack location which maximize $G^*_{A_1}$, $G^*_{A_2}$ are $x\fallingdotseq 0.8$ for SiC, $x\fallingdotseq 0.5$ for Stellite and $x\fallingdotseq 0.2$ for Al_2O_3.

Then, in order to investigate the mutual interference effects of the cracks, the maximum energy release rate ($G^*_{A_1\,\max}$, $G^*_{A_2,\max}$) are shown in Figs. 5 and 6 as functions of the distance d^* between the two cracks for the various frictional coefficients ($f=0.1$, 0.3, 0.7) and the various heat input parameters ($\lambda=0.0$, 0.5, 1.0, 1.5), respectively. From these figures, we can recognize the effect of mutual interference of the cracks; that is, the values of $G^*_{A_1,\max}$, $G^*_{A_2,\max}$ increase with a decrease of the distance d^* between the cracks. Especially, $G^*_{A_2,\max}$ (at the inside tip) show a marked interference effect compared with $G^*_{A_1,\max}$ (at the outside tip). In these figures, the results of single crack are also shown by the symbols (○△▽□) being the crack length $l=2l_1=2l_2=0.1$, and the symbols (●▲▼■) being the crack length $l=2l_1+2l_2=0.2$. As the distance d^* increase, the results of $G^*_{A_1,\max}$, $G^*_{A_2,\max}$ coincide with the results of the single crack which are shown by the symbols (○△▽□). In fact, when two cracks go away from each other at a distance $d^*>0.5$, instead of those results of $G^*_{A_1,\max}$, $G^*_{A_2,\max}$ the results of the single crack can be used. While, as the distance d^* decrease, the results of $G^*_{A_1,\max}$ at the crack tip A_1 seem to approach to the results of single crack which are shown by the symbols (●▲▼■), however the results of $G^*_{A_2,\max}$ at the crack tip A_2 are always greater than those results of single crack shown by the symbols (●▲▼■). From Fig. 5, the values of $G^*_{A_1,\max}$, $G^*_{A_2,\max}$ increase with an increase of frictional coefficient f (up to $f=0.7$) regardless of the distance d^*. Especially, this tendency is extremely sensitive for the case of SiC-coating. Similarly, from Fig. 6 the values of $G^*_{A_1,\max}$, $G^*_{A_2,\max}$ increase with an increase of heat input strength λ (up to $\lambda=1.5$) regardless of d^*. Especially, this tendency is extremely sensitive for the case of the coating by Stellite which has the smallest value of thermal conductivity within the three kinds of coating materials as shown in Table 1.

Next, the effects of the layer thickness h on the energy release rate and on their mutual interference are considered. Figure 7 shows the maximum energy release rates at the crack tip $A_2(G^*_{A_2,\max})$ as a function of the distance d^* between the two cracks for the various layer thickness ($h=0.1$, 0.3, 0.5), for the case of $f=0.1$ and $\lambda=1.2$. In this figure, the results of single crack are also shown by the same symbols as Figs. 5 and 6. From this figure, we can recognize the same mutual interference effect as Figs. 5 and 6 for any layer thickness ($h=0.1\sim0.5$). In order to estimate the mutual interference effect quantitatively, Fig. 8 shows the ratio $(G^*_{A_2,\max})_{d^*=0.01}/(G^*_{A_2,\max})_{d^*=\infty}$ as a function of layer thickness h for the case of $f=0.1\sim0.7$, $\lambda=0.0\sim1.2$ and three kinds of coating materials which we have been considered here. Where, $(G^*_{A_2,\max})_{d^*=0.01}$

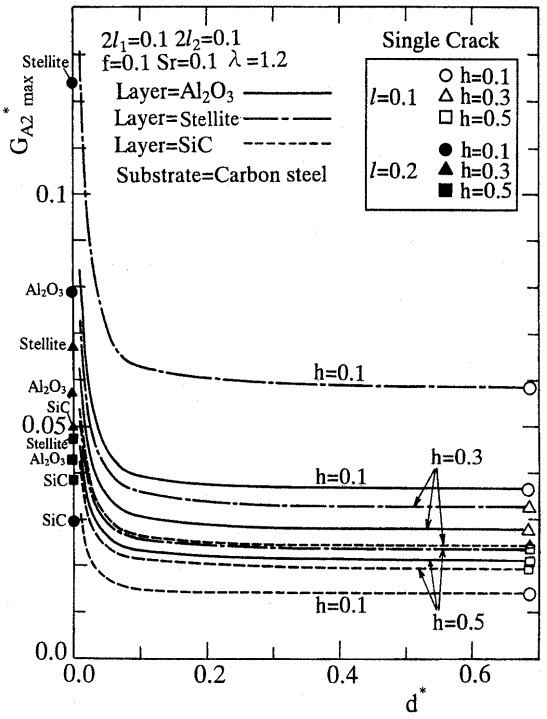

Fig. 7 Interference effects on the maximum energy release rate with a decrease of the distance between the two cracks for the various values of layer thickness h=0.1, 0.3 and 0.5

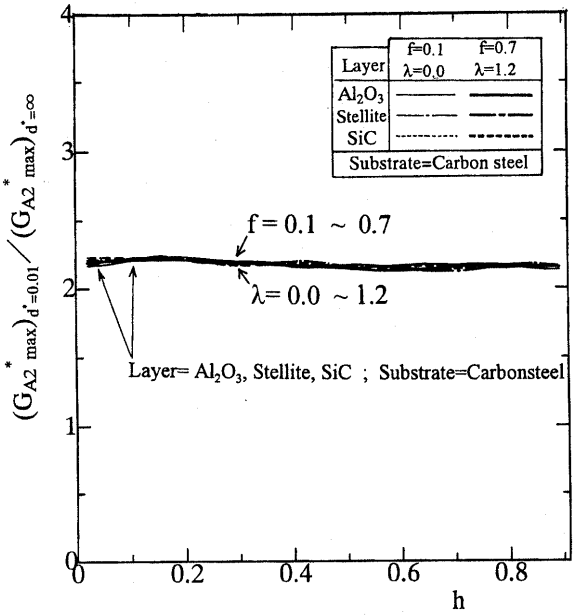

Fig. 8 The ratio of the maximum energy release rate for d^*=0.01 and for d^*=0.5 as functions of layer thickness h

represent the energy release rate for d^*=0.01 and $(G^*_{A2,\max})_{d^*=\infty}$ represent for the single crack. These ratios for various case are almost equal within the range 2.15~2.25 as shown in Fig. 8. Therefore, approximately we can assume $(G^*_{A2,\max})_{d^*=0.01}/(G^*_{A2,\max})_{d^*=\infty} \fallingdotseq 2.2$, regardless frictional coefficient, heat

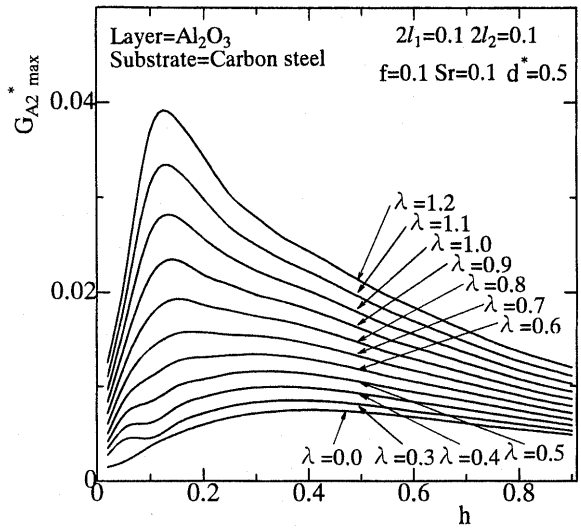

Fig. 9 Maximum energy release rates as functions of the layer thickness h showing the effect of heat input strength for the case of Al_2O_3-coating

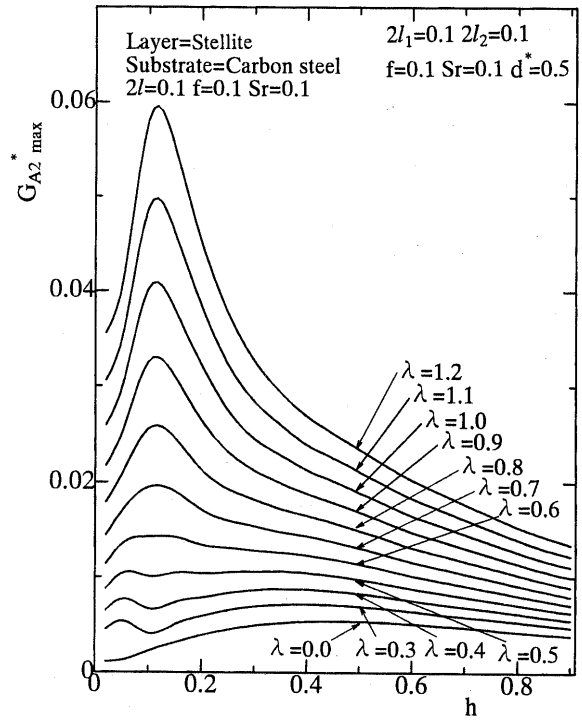

Fig. 10 Maximum energy release rates as functions of the layer thickness h showing the effect of heat input strength for the case of Stellite-coating

input strength, layer thickness, and the properties of coating materials which we mentioned above. Hence, the energy release rate $(G^*_{A2,\max})_{d^*=0.01}$ for two cracks (d^*=0.01) can be estimated approximately by using the results of single crack as $2.2(G^*_{A2,\max})_{d^*=\infty}$. Again, from Fig. 7, the value of $G^*_{A2,\max}$ increase with a decrease of the layer thickness h (from 0.5 to 0.1) for the case of Al_2O_3 and Stllite coating materials. However, for the case of SiC coating $G^*_{A_2,\max}$ show the

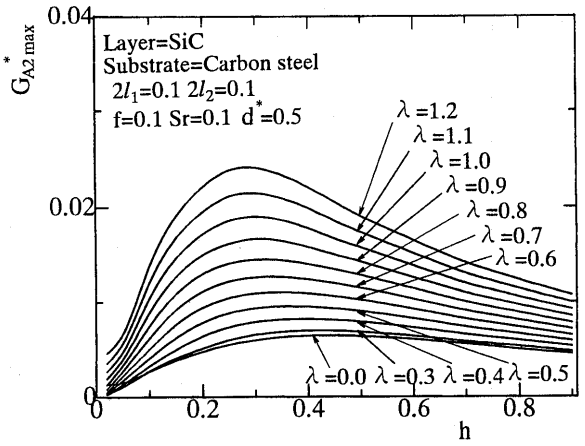

Fig. 11 Maximum energy release rates as functions of the layer thickness h showing the effect of heat input strength for the case of SiC-coating

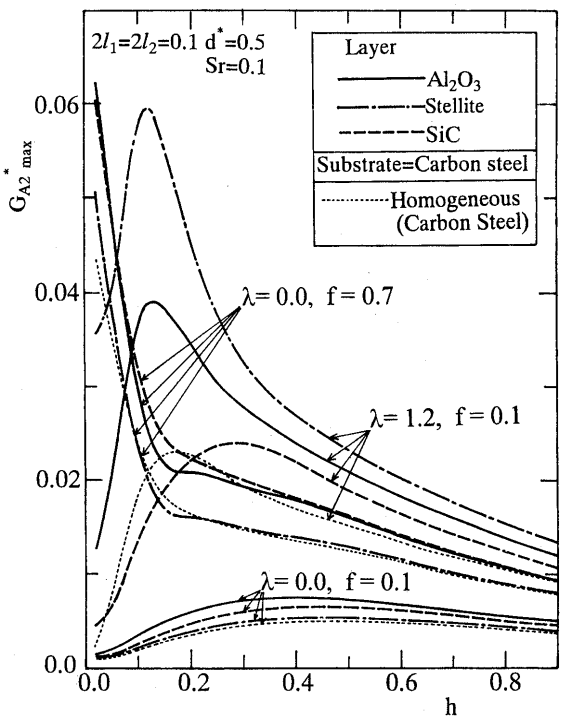

Fig. 12 Maximum energy release rates as functions of the layer thickness h showing the comparison of thermal effect with frictional effects

maximum value at h=0.3.

Therefore, in the following figure, the thermal effects on the layer thickness which maximize the value of $G^*_{A2,\max}$ are investigated. Figures 9, 10 and 11 show the variation of $G^*_{A2,\max}$ by the layer thickness h accompanied by the change with heat input parameter λ=0.0～1.2 (being f=0.1, d^*=0.5), for each cases of Al_2O_3, Stllite and SiC coatings respectively. From these figures, we can see that $G^*_{A2,\max}$ increase with an decrease of layer thickness (starting from h=0.9), and attain a maximum at a certain value of h(0.45～0.1) for each value of λ(0.0～1.2) and coating materials. Then, if we designate the layer thickness which maximize the value of $G^*_{A2,\max}$ by $h_{\max}$, for the case of λ=0.0 (no heat input) and f=0.1, the layer thickness $h_{\max}\fallingdotseq$0.5 is obtained independent of the properties of coating materials. However, the values of $h_{\max}$ decreases with an increase of λ. For example, for the case of λ=1.2, $h_{\max}\fallingdotseq$0.12 for Al_2O_3 coating (Fig. 9), $h_{\max}\fallingdotseq$0.115 for Stellite coating (Fig. 10) and $h_{\max}\fallingdotseq$0.28 for SiC coating (Fig. 11). The results in Figs. 9-11 were only for the case of f=0.1. Therefore, Fig. 12 shows the comparison of thermal effects with frictional effects on those variations. Three representative examples (f=0.7, λ=0.0), (f=0.1, λ=0.0) and (f=0.1, λ=1.2) are shown for three kinds of coating materials. In the same figure, the results of energy release rate for the coordinately located subsurface cracks in the homogeneous carbon steel half-space which has no coating layer, are also shown by the dotted curve. From this figure, for the case of large frictional coefficient (f=0.7), the value of $G^*_{A2,\max}$ rapidly increase with decreasing the layer thickness h(<0.2). In all cases, the results of $G^*_{A2,\max}$ are always greater than the homogeneous ones which are shown by the dotted curve.

6. Conclusions

This work has analyzed the energy release rate for multiple interface cracks in a surface layered material due to rolling-sliding contact with heat input. From numerical examples of the energy release rate for a pair of interface cracks and for three kinds of coating materials (Al_2O_3, Stellite and SiC) being carbon steel substrate, the following conclusions can be made.

(1) The maximum values of energy release rate increase with increasing of frictional coefficient f and heat input strength λ. Especially, these tendencies are remarkable for the case of SiC-coating (by increasing of f) and Stellite-coating (by increasing of λ), respectively.

(2) The magnitudes of energy release rate increase with decreasing distance between the two cracks due to the mutual interference by the cracks. The energy release rates at the inside tip show a marked interference effect compared with at the outside tip. Their increasing rate to the results of single crack are approximately constant which are not affected very much by the change of f, λ and the properties of coating materials.

(3) The ratio of the layer thickness and the half contact length which maximize the energy release rate is about $h_{\max}\fallingdotseq$0.45 for the case of small frictional coefficient (f=0.1) and no heat input (λ=0) and that

is independent of the properties of coating materials. However, these ratios h_{max} decrease with increasing of frictional coefficient and heat input strength and they are dependent on the properties of coating materials.

(4) In the present numerical examples, the results of energy release rate for interface crack in layered media are always greater than those for the equally located subsurface cracks in the homogeneous carbon steel half-space.

References

(1) Ju, F.D. and Chen, T.Y., Thermomechanical Cracking in Layered Media From Moving Friction Load, Trans. ASME, J. Tribol., Vol. 106 (1984), p. 513-518.

(2) Ju, F.D. and Liu, J.C., Parameters Affecting Thermomechanical Cracking in Coate Media Due to High-Speed Friction Load, Trans. ASME, J. Tribol., Vol. 110 (1988), p. 222-227.

(3) Chen, T.Y. and Ju, F.D., Friction-Induced Thermomechanical Cracking in a Coated Medium With a Near Surface Cavity, Trans. ASME, J. Tribol., Vol. 111 (1989), p. 270-277.

(4) Leory, J.M., Floquet, A. and Villechaise, B., Thermomechanical Behavior of Multilayered Media: Theory, Trans. ASME, J. Tribol., Vol. 111 (1989), p. 538-544.

(5) Chen, L.S. and Chu, H.S., Transient Thermal Stresses Due to Periodic Moving Frictional Load in Layered Media, J. Thermal Stresses, Vol. 12 (1989), p. 169-189.

(6) Goshima, T. and Takayama, H., Thermomechanical Cracking in a Surface Layered Medium due to Rolling Contact with Frictional Heating, Proceedings of the 1st International Symposium on Thermal Stresses and Related Topics, (1995), p. 67-70.

(7) Goshima, T., Nishino, T. and Koizumi, T., Thermomechanical Effects due to Rolling Contact on an Interface Crack Growth in a Surface Layered Material, Proceedings of the 2nd International Symposium on Thermal Stresses and Related Topics, (1997), p. 11-14.

(8) Mulville, D.R. and Mast, P.W., Strain Energy Release for Interfacial Cracks Between Dissimilar Media, Eng. Fract. Mech., Vol. 8 (1976), p. 555-565.

(9) Ju, F.D. and Liu, J.C., Effect of Peclet Number in Thermo-Mechanical Cracking due to High-Speed Friction Load, Trans. ASME, J. Tribol., Vol. 110 (1988), p. 217-221.

(10) Dundurs, J., Elastic Interaction of Dislocations with Inhomogeneities, Mathematical Theory of Dislocations, (1975), p. 70-115, ASME Publication.

(11) Miller, G.R. and Keer, L.M., A Numerical Technique for the Solution of Singular Integral Equation of the Second Kind, Q. Appl. Math., Vol. 42 (1985), p. 455-465.

(12) Hutchinson, J.W., Mear, M.E. and Rice, J.R., Crack Paralleling an Interface Between Dissimilar Materials, Trans. ASME, J. Appl. Mech., Vol. 54 (1987), p. 828-832.

(13) Sun, C.T. and Jih, C.J., On Strain Energy Release Rates for Interfacial Cracks in Bi-Material Media, Eng. Fract. Mech., Vol. 28, No. 1 (1987), p. 13-20.